Hierarchical Nanocomposites of Polyaniline Nanowire Arrays on Graphene Oxide Sheets with Synergistic Effect for Energy Storage

Jingjing Xu,[†] Kai Wang,[†] Sheng-Zhen Zu, Bao-Hang Han,* and Zhixiang Wei*

National Center for Nanoscience and Technology, No. 11 Beiyitiao, Zhongguancun, Beijing 100190, China. [†]These authors contributed equally to this work.

ABSTRACT We introduced a facile method to construct hierarchical nanocomposites by combining one-dimensional (1D) conducting polyaniline (PANI) nanowires with 2D graphene oxide (GO) nanosheets. PANI nanowire arrays are aligned vertically on GO substrate. The morphologies of PANI nanowires can be controlled by adjusting the ratios of aniline to GO, which are attributed to different nucleation processes. The hierarchical nanocomposite structures of PANI—GO were further proved by UV—vis, FTIR, and XRD measurements. The hierarchical nanocomposite possessed higher electrochemical capacitance and better stability than each individual component as supercapacitor electrode materials, showing a synergistic effect of PANI and GO. This study will further guide the preparation of functional nanocomposites by combining different dimensional nanomaterials.

KEYWORDS: hierarchical · nanocomposite · conducting polymer · graphene oxide · supercapacitor

Combining unique properties of individual nanostructures and possibly synergistic effects, nanocomposites have attracted great attention ranging from biosensing to energy conversion and storage.[1−6] Therefore, by function-oriented selection of nanocomponents, hierarchical nanocomposites with high performance are highly expected. Focusing on this aim, composition of one-dimensional (1D) nanowires (or nanotubes) with zero-dimensional (0D) nanoparticles has been extensively studied, which can be applied in electronics, optoelectonics, and catalysis.[7−9] Recently, with extensive studies on two-dimensional (2D) graphene nanosheets, composition of 2D nanosheets with 0D nanoparticles has also been reported in a few cases.[10,11] However, there is almost no report on constructing hierarchical nanocomposites by combining 2D nanosheets with 1D nanowires.

Herein, we report a novel hierarchical nanocomposite of conducting polyaniline (PANI) nanowire arrays grown vertically on graphene oxide sheets. Graphene-based materials have shown promising application in nanoelectronics and energy storage recently. Due to their high specific surface area and excellent conductivity, graphene is a promising electrode material for supercapacitors.[12−14] However, the capacitance of carbon materials is ascribed to the electrical double layer at an electrode/electrolyte interface, which is highly dependent on the specific area of the electrode.[15,16] Due to unavoidable aggregation of graphene nanosheets, graphene-based nanomaterials exhibited unsatisfactory capacitance performance, generally 100−200 F/g.[17,18] Compared with carbon materials, conducting polymers show much higher capacitance due to the pseudocapacitance of the redox reaction of electrode material.[19−24] However, the poor cycle life limits their real application in supercapacitors. In order to avoid the drawback of single material and to obtain materials with both high capacitance performance and good cycle life, researchers are striving to develop synergistic composite materials.[3−5,14]

In this article, hierarchical nanocomposites of PANI nanowire arrays on graphene oxide (GO) sheets are successfully obtained, which show a synergistic effect used as the supercapacitor electrode materials. The specific capacitance of the nanocomposite can reach as high as 555 F/g at a discharge current density of 0.2 A/g, which is much higher than 298 F/g of random connected PANI nanowires obtained in the same conditions. In addition, the cycle life of this composite is also much better than that of random connected PANI nanowires. It indicated that, by optimizing the composition of different materials at the nanoscale,

*Address correspondence to weizx@nanoctr.cn, hanbh@nanoctr.cn.

Received for review March 31, 2010 and accepted August 18, 2010.

Published online August 26, 2010.
10.1021/nn1006539

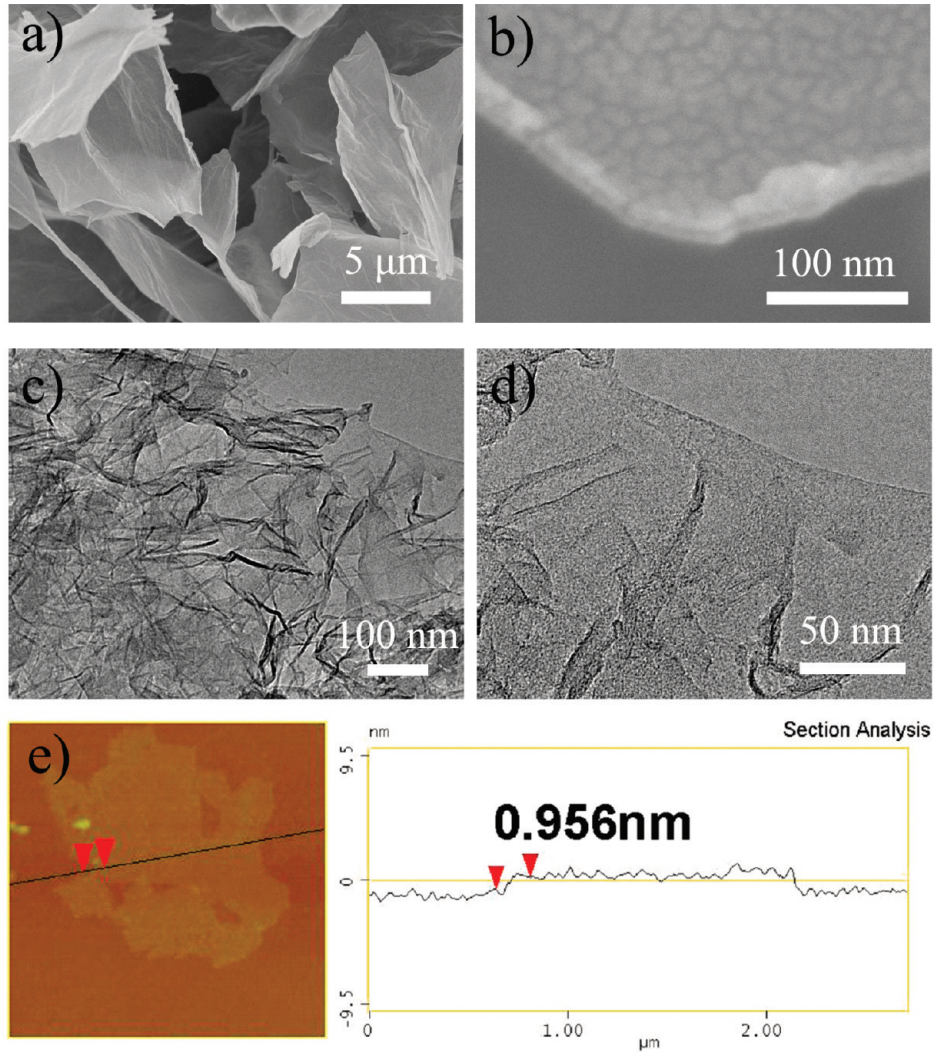

Figure 1. SEM, TEM, and AFM images of GO sheets. (a) Low- and (b) high-magnification SEM images of GO. Au ion sputtering was carried out before SEM because of the poor conducting property of separated GO sheets. The Au layer can be observed clearly in image (b), and the GO nanosheet is sandwiched between Au layers. (c) Low- and (d) high-magnification TEM images showing the layer morphology of graphene oxide. (e) AFM image of GO on mica and its section analysis

a significant synergistic effect was achieved for energy storage.

RESULTS AND DISCUSSION

Preparation of Hierarchical Nanocomposites by Controlling the Nucleation Process. It has been reported that, compared with random connected nanowires, well-ordered nanostructure can reduce the ionic diffusion path, facilitate ionic motion to the inner part, and improve utilization of electrode materials. Therefore, nanowire and nanotube arrays have been successfully used as supercapacitor electrode material.[3,4] However, nanostructure arrays were produced on bulky substrates in most cases, which creates the problem of increasing the quantities of electrode materials in the real applications. In order to utilize the advantages but to avoid the drawbacks of nanostructure arrays, we selected GO nanosheets as substrates to produce PANI nanowire arrays. GO nanosheet is a two-dimensional carbon nanomaterial with many merits, such as low manufacturing cost, facile mass production, and remarkable mechanical behavior.[25,26] Moreover, there are many oxygen-containing functional groups on the surface of GO, which makes it easily dispersed in aqueous solution and may act as the nucleation sites for producing PANI nanowire arrays.[27]

Aqueous GO solution was produced from natural flake graphite (100 mesh) by a modified Hummers method, in which GO existed in single or a few layer structure.[25,26] SEM images of GO (Figure 1a,b) also showed 2D nanosheet morphologies. In order to avoid the aggregation of GO in the dry process, the sample was obtained by freeze-drying. Normal drying process produced aggregated GO layers, as shown in the Supporting Information (Figure S1). Besides, the Au ion sputtering on the sample was employed due to the poor conductive property of GO. The Au nanoparticle layer with a thickness of *ca.* 20 nm could be clearly observed on both sides of GO sheet, as shown in Figure 1b. From the cross section investigated by SEM, the

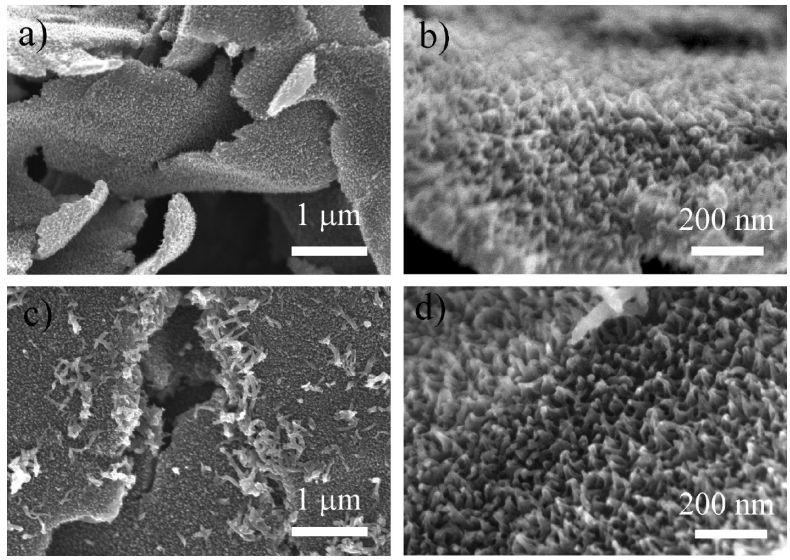

Figure 2. SEM images of PANI−GO nanocomposites at different concentration of aniline: (a,b) 0.05 M; (c,d) 0.06 M. Other conditions: aniline/APS = 1.5 (molar ratio), $HClO_4$ = 1 M, GO = 0.36 mg/mL, and the reaction was carried out at −10 °C for 24 h.

thickness of GO sheets is about 20 nm, but this thickness is mainly contributed from Au nanoparticles. Transmission electron microscopy (TEM) was further used to confirm the nanosheet morphology of graphene oxide. From TEM images in Figure 1c,d, the curly layer morphology of graphene oxide sheets is clearly shown. From the atom force microscopy (AFM) image, the thickness of most graphene oxide sheets was *ca.* 1.0 nm (Figure 1), which fit well with the thickness of an individual layer of GO.[26]

The aligned PANI nanowires were produced by dilute polymerization of aniline monomer in the GO aqueous solution. Polymerization of aniline in its dilute solution has been successfully used for the preparation of PANI nanowire arrays on various bulky substrates.[28] In our study, we expected that PANI nanowire arrays could be produced vertically aligned on GO nanosheets that dispersed in the aqueous solution. As shown in Figure 2a,b, hierarchical PANI nanowire arrays on the GO nanosheet were successfully prepared at −10 °C. The temperature affected the morphologies of PANI nanowires, which would have an improved uniformity under a low polymerization temperature based on our experiments. PANI nanowire arrays were evenly covered on GO sheets, indicating that the nucleation and growth processes only occurred on the surface of GO sheets. In our experiments, morphologies of PANI−GO nanocomposites were highly affected by the ratio of aniline monomer to GO. At a constant concentration of GO (0.36 mg/mL), the optimized concentration of aniline was 0.05 M. Lower concentration of aniline (*e.g.*, 0.01−0.04 M) resulted sparser and shorter PANI nanowires than that obtained at 0.05 M. On the other hand, self-nucleation of PANI was unavoidable at a higher concentration of aniline (*e.g.*, 0.06 M), and thus both random connected PANI nanowires and aligned PANI nanowires were produced (Figure 2c,d).

On the basis of the above experimental results, a formation mechanism of PANI−GO nanocomposites is illustrated in Figure 3. In the chemical oxidation polymerization process of polyaniline, two possible nucleation sites (that is, bulky solution and solid substrates) compete with each other. When *dilute* aniline is employed (less than 0.05 M), most active nucleation sites were generated on the GO nanosheet surface at the beginning of the polymerization process by heterogeneous nucleation. These active sites would minimize the interfacial energy barrier between the solid surface and bulk solution, which was beneficial to the subsequent growth of polyaniline on the solid substrates.[28] Moreover, the low concentration of aniline cannot reach a supersaturation state so that the homogeneous nucleation was suppressed. PANI nanowires would further grow along the initial nuclei, and therefore, aligned PANI nanowires on GO nanosheets were produced. However, when the concentration aniline was higher (*e.g.*, 0.06 M), homogeneous nucleation will take place after the initial nucleation on the solid surface.[29] Consequently, homogeneous nucleation will produce random connected PANI nanowire by using aniline micelles as "soft template".[30] As a result, two morphologies of PANI nanowires were produced, that is, random connected PANI nanowires from homogeneous nucleation in bulk solution and aligned PANI nanowires from heterogeneous nucleation on the GO nanosheet.

To further prove the formation process of a hierarchical nanocomposite, PANI−GO samples were taken out from the reaction solution at different time intervals during the polymerization process (the concentration of aniline was 0.05 M). As displayed in Figure 4a, GO nanosheets still looked smooth after 2.5 h polymeriza-

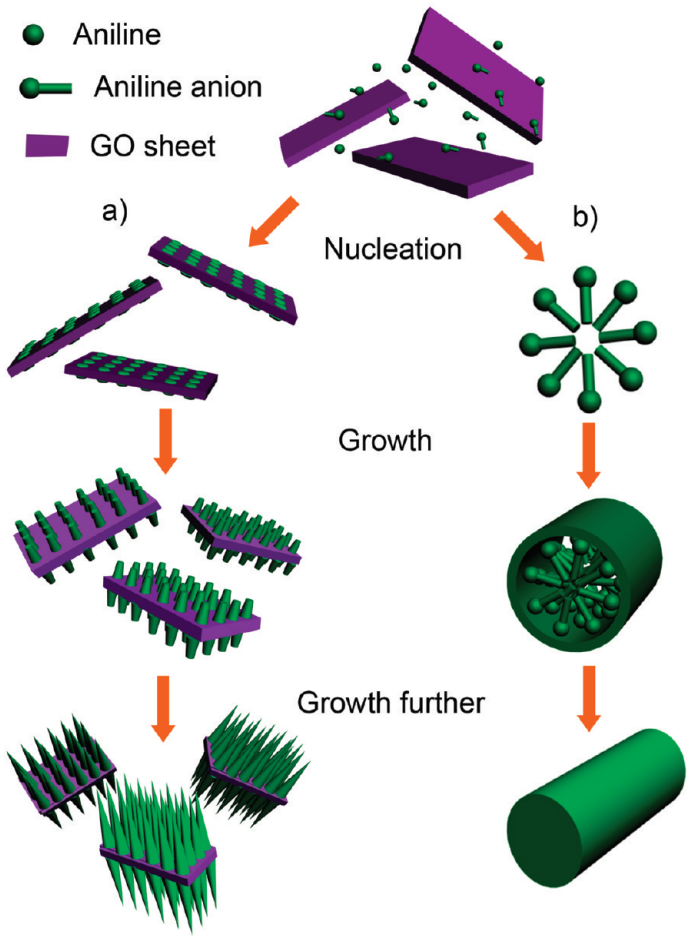

Figure 3. Schematic illustration of nucleation and growth mechanism of PANI nanowires: (a) heterogeneous nucleation on GO nanosheets; (b) homogeneous nucleation in bulk solution.

tion. However, after a reaction time of 3 h, some protuberances appeared on the surface of GO sheets (Figure 4b), which indicated that a large number of PANI nuclei were produced. GO has two-dimensional sheets that have various oxygen functional groups (*e.g.*, hydroxyl, epoxy, and carbonyl groups) on their basal planes and edges. These functional groups act as anchor sites and enable the subsequent *in situ* polymerization of PANI attaching on the surfaces and edges of GO sheets.[31] Besides, the π−π stacking force between the phenyl and basal planes of GO was also beneficial to *in situ* polymerization occurring on the surface of GO. Therefore, the PANI would gradually grow along the initial nuclei of PANI and form long nanowire arrays (Figure 4c,d) at a dilute solution and a low reaction temperature.

Structural Characterization of Hierarchical Nanocomposites. The structures of pristine GO, PANI−GO nanocomposite, and random connected PANI nanowires (prepared at 0.05 M of aniline) were characterized by the Fourier transformed infrared (FTIR) spectra, UV−vis spectra, elemental analysis, and X-ray diffraction (XRD). Elemental analysis was used to examine the components of the PANI−GO nanocomposite. The results revealed that the weight ratio of C, N, and Cl elements were 47.96, 8.04, and 10.66%, respectively. From the weight ratio of N and Cl elements, it can be calculated that the molar ratio of N and ClO_4^- groups was *ca.* 0.5, indicating the doping degree of PANI was *ca.* 50%. In addition, the weight ratio of C and N in the nanocomposite (5.96) is higher than that in doped PANI (5.14), from which we calculated that the weight content of GO was *ca.* 8.7% in the PANI−GO nanocomposite. The measured content of GO was higher than the feeding amount (7.2%) in the reactants. This was mainly due to oligomers of aniline produced in the polymerization, and these oligomers can be washed away by methanol in the post-treatment process.

The composite structure was further proved by spectroscopy measurement. In the FTIR spectrum of GO, the peaks around 3385, 1727, 1635, and 1405−1057 cm^{-1} are attributed to the O−H, C═O in COOH, intercalated water, and C−O in C−OH/C−O−C functional groups, respectively.[32,33] Compared with GO,

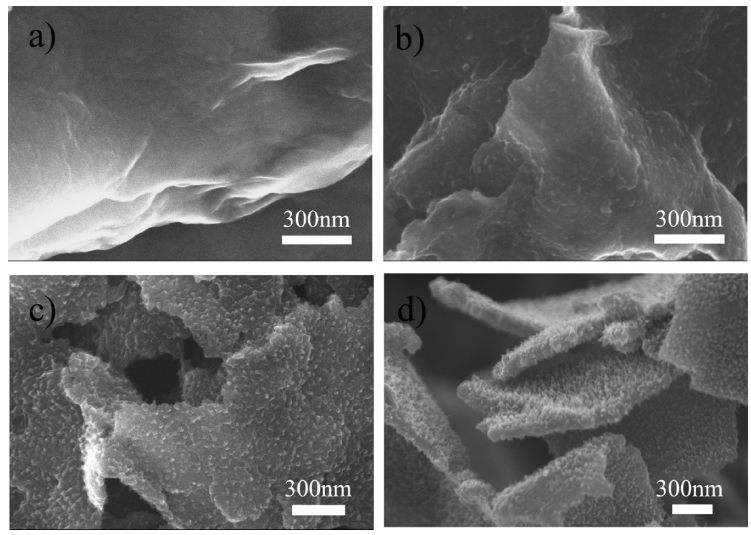

Figure 4. SEM images of PANI−GO samples obtained at different reaction intervals: (a) 2.5 h, (b) 3 h, (c) 8 h, and (d) 24 h.

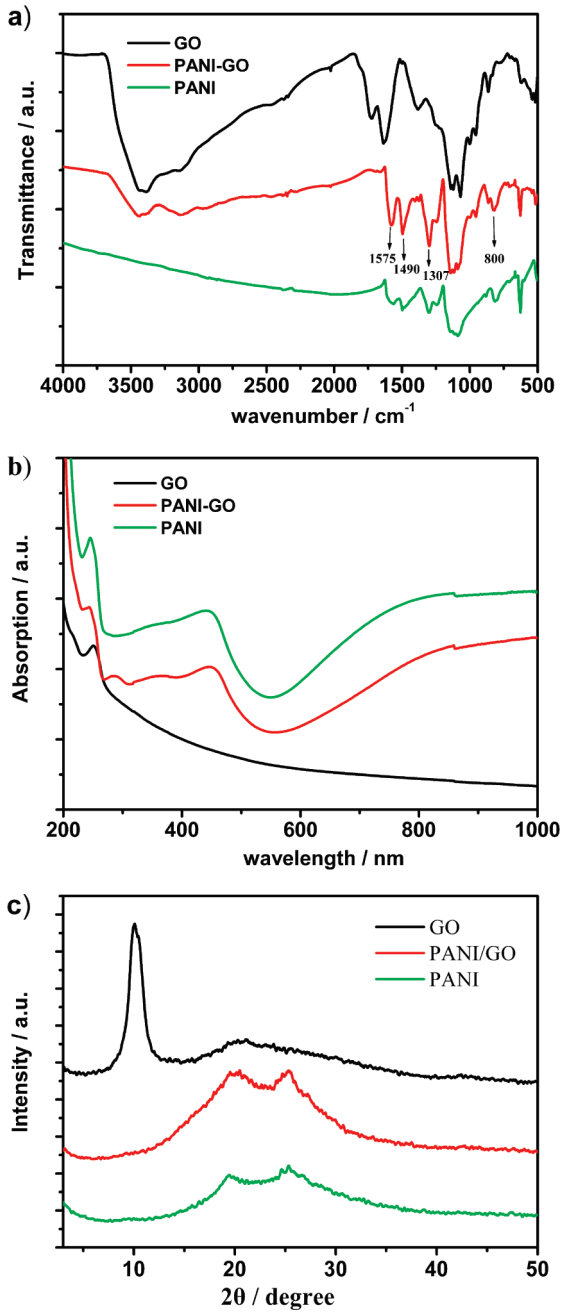

Figure 5. (a) FTIR, (b) UV−vis, and (c) XRD spectra of pristine GO, random connected PANI nanowires, and PANI−GO nanocomposite.

several new peaks attributed to PANI appeared in the spectrum of PANI−GO (Figure 5a). The new peaks at 1575, 1490, 1307, and 800 cm^{-1} are attributed to the vibration of C═N, C═C, C−N, and C−H, respectively.[34−36] Moreover, in the UV spectra of the PANI−GO nanocomposite displayed in Figure 5b, besides the absorption at 250 nm from GO, there are two new absorption bands at 450 and 800 nm with a free-tail extended to the IR region, respectively. They are attributed to the absorption of PANI and could be assigned to the polaron transition, which is a typical characterization of conducting state PANI.[37,38] Therefore, PANI in the nanocomposite is highly doped, which will be beneficial to the supercapacitor properties.

The PANI nanowire loaded on the GO nanosheet could be further confirmed by X-ray diffraction (XRD), as shown in Figure 5c. XRD patterns of the pristine GO revealed an intense, sharp peak centered at $2\theta = 10.04°$, corresponding to the interplanar spacing of 0.88 nm of GO sheets.[39] In the case of PANI−GO, the peak of GO stacking disappeared, indicating the GO had almost no aggregation and was fully used as the substrate of PANI nanowires to produce hierarchical nanocomposites. Two new broad peaks of PANI−GO centered at $2\theta = 20.12$ and 25.26° are almost the same as that of pure PANI nanowires, which are the characteristic Bragg diffraction peaks of PANI.[40]

Hierarchical Nanocomposite for Energy Storage. As with the well-aligned doping state of PANI nanowires, composite materials of PANI−GO are expected to show excellent performance as supercapacitor electrode materials. Above all, the influence of aniline concentration on the capacitance property was systematically investigated by galvanostatic charge/discharge (0.5 A g^1). As shown in Figure 6, the specific capacitance of PANI−GO increased with the concentration of aniline from 0.01 to 0.05 M, until as high as 555 F/g at 0.05 M aniline. That is because aligned PANI nanowires get denser with the increase of aniline concentration. As the concentration of aniline further increased to 0.06 M, however, the specific capacitance of PANI−GO decreased to 392 F/g. It is noticed that random connected PANI nanowires were also produced besides aligned PANI nanowires at the concentration of 0.06 M. Those random connected PANI nanowires were not fully used for energy storage and might act as artifacts to lower the capacitance property of PANI−GO nanocomposite.

To further confirm the merits of PANI−GO nanocomposite as a supercapacitor electrode, the electrochemical properties of PANI, GO, and PANI−GO (prepared at 0.05 M of aniline) were fully characterized by cyclic voltammetry (CV), electrochemical impedance spectroscopy (EIS), galvanostatic charge/discharge, and cycling life measurement. In their CV curves (Figure 7a), there was nearly no peaks for GO and two pairs of redox peaks appeared for PANI−GO and pristine PANI, which were attributed to two redox transitions of PANI (*i.e.*, the leucoemeraldine−emeraldine transition and the emeraldine−pernigraniline transition). Therefore, the capacitance of PANI−GO mainly comes from Faradaic reactions of PANI at the electrode/electrolyte surface, which is different from that of the electric double-layer capacitance of carbon-based materials. Galvanostatic charge/discharge plots (at 1 A/g) of PANI and PANI−GO nanocomposite in Figure 7b showed a capacitive behavior with almost symmetric charge−discharge curves. Moreover, the small deviation to linearity is typical of a pseudocapacitive contri-

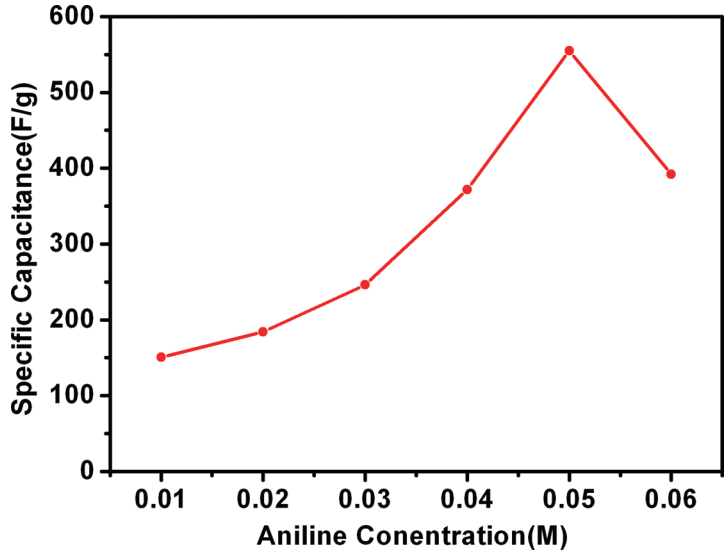

Figure 6. Influence of aniline concentration on the specific capacitance of PANI−GO.

bution, which showed that the capacitances of PANI and PANI−GO nanocomposite mainly originate from pseudocapacitance. The specific capacitance of both samples decreased with increasing discharge current densities (Figure 7c), but the capacitance of PANI−GO was always higher than that of PANI in all current densities. The specific capacitance of PANI−GO was 555 F/g at a discharge current of 0.2 A/g and was still kept as high as 227 F/g even at a discharge current density of 2 A/g. Compared to disordered PANI nanowires (see Figure S2 in Supporting Information), PANI nanowires in the nanocomposite have much smaller diameters (*ca.*

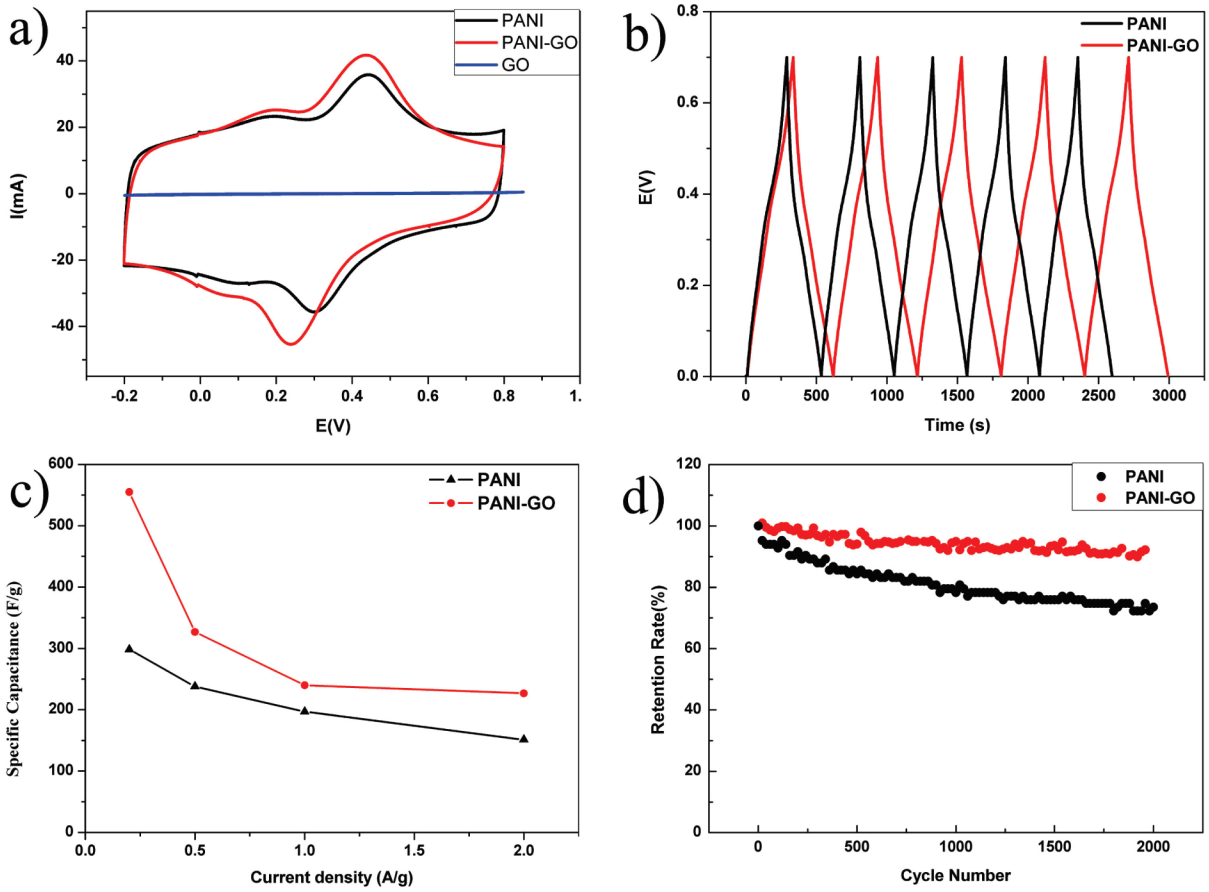

Figure 7. Electrochemical capacitance performance of PANI−GO obtained at 0.05 M of aniline. (a) CV curves of pristine GO, random connected PANI nanowires, and PANI−GO, nanocomposite within the potential window −0.2 to 0.8 V *vs* SCE at a scan rate of 20 mV s^{1}; (b) charge−discharging curves of PANI and PANI−GO; (c) specific capacitance of PANI and PANI−GO at different current densities; (d) stability of PANI and PANI−GO.

50 nm) and an optimized ionic transport pathway, which led to an improved capacitance performance. The Nyquist plots of both samples (see Figure S3 in Supporting Information) showed almost a straight line in the low-frequency region that exhibited an ideal capacitive behavior. In the high-frequency region, they showed an inconspicuous semicircle which was related to the reduced electrical charge transfer resistance. From Nyquist plots, it was obvious that PANI−GO showed low charge transfer resistance and ideal capacitive behavior just like pristine conducted PANI.

In general, conducting polymers often suffer from a limited long-term stability during cycling because the swelling and shrinking of the polymers may lead to degradation, which restricts these low-cost supercapacitor electrode materials for commercial application. However, the composition with GO is able to meliorate this situation noticeably. The electrochemical stability of PANI−GO was examined in 1 M H_2SO_4 aqueous electrolyte by consecutive charge−discharge cycles at a current density of 1 A/g (Figure 7d). Interestedly, PANI−GO nanocomposite exhibited a much higher stability than random connected PANI nanowires. For instance, after 2000 consecutive cycles, the capacitance retention of PANI−GO nanocomposite still kept 92% of its initial capacitance, while pristine PANI kept only 74% of its initial capacitance. The better stability of PANI−GO came from the synergistic effect of GO and PANI nanowire arrays. GO nanosheets undertook some mechanical deformation in the redox process of PANI nanowires, which avoided destroying the electrode material and was benefited to a better stability. Besides, the vertical nanowire arrays were facile to strain relaxation, which allowed them to decrease the breaking during the doping/dedoping process of counterions.[23,24] Therefore, the PANI−GO nanocomposite showed an enhanced cyclic stability over random connected nanowires as supercapacitor electrode materials.

CONCLUSIONS

In summary, aligned PANI nanowires are delicately synthesized on two-dimensional GO nanosheets by dilute polymerization. The morphologies of PANI nanowires can be controlled by adjusting the ratio of aniline to GO, which are attributed to different nucleation processes. At suitable concentration of aniline (0.05 M), heterogeneous nucleation on GO nanosheets was dominated, and uniform aligned PANI nanowire arrays on GO nanosheet was obtained with a high yield. The electrochemical studies proved that PANI−GO nanocomposite possessed a synergistic effect of PANI and GO, which showed higher electrochemical capacitance and better stability than each individual component. This study introduces a facile method to construct a hierarchical nanocomposite using 1D and 2D nanocomponents and may guide the way for designing new composite materials at the nanoscale level.

METHODS

Preparation of PANI−GO Nanocomposites. GO was synthesized from natural flake graphite (100 mesh) by Hummers method.[25,26] PANI−GO nanocomposites were synthesized by dilute polymerization in the presence of GO and aniline monomer. In a typical procedure, aqueous GO solution (containing 9 mg of GO) was added into 15 mL of 1 mol/L aqueous $HClO_4$ solution, and the mixture was ultrasonicated until GO was fully dispersed. Afterward, 5 mL of ethanol was added into the reaction solution in order to avoid the solution being frozen. Then aniline monomer was added into the above solution and stirred for 30 min at −10 °C to form a uniform mixture. The oxidant, $(NH_4)_2S_2O_8$ (APS), was dissolved in 5 mL of aqueous $HClO_4$ solution (the molar ratio of aniline/APS is 1.5) and cooled to −10 °C. The polymerization was performed by rapid addition of the precooled oxidant solution, and the mixture was stirred for 24 h at −10 °C. An emerald flocculent precipitate was obtained and filtered and washed with a large amount of 0.1 mol/L $HClO_4$, methanol, and ether. The product was dried at 45 °C for 24 h under vacuum. For comparison, random connected PANI was synthesized chemically at 0.05 M aniline in the absence of graphene oxide *via* the similar procedure above.

Characterization. The as-prepared samples were characterized by SEM (Hitachi S-4800), TEM (Tecnai G220 S-TWIN TEM operating at 200 kV), FTIR spectroscopy (Spectrum One), UV−vis spectroscopy (PE Lambda 650/850/950), and rotation anode X-ray powder diffraction (Rigaku D/max-2500) equipped with graphite monochromatized Cu Kα radiation.

Electrochemical Performance Measurement. Electrochemical measurements were carried out using two-electrode sandwich-type construction cells with a glassy fibrous separator between the two symmetrical working electrodes. A gold grid was used as current collector. The mixture containing 85 wt % active material, 10 wt % conducting carbon black, and 5 wt % polytetrafluoroethylene (used as a binder, PTFE 60% dispersion in H_2O, Sigma Aldrich) was well mixed and then pressed onto the gold grid (1.0×10^7 Pa). The electrochemical performances of the prepared electrodes were characterized by cyclic voltammetry (CV), electrochemical impedance spectroscopy (EIS) measurements, and galvanostatic charge−discharge tests. The used electrolyte was 1 mol/L aqueous H_2SO_4 solution. The experiments were performed using an EG&G Princeton Applied Research VMP3 workstation controlled by a computer.

Acknowledgment. We acknowledge the financial support of the National Natural Science Foundation of China (Grants 20974029 and 20972035), The Ministry of Science and Technology of China (2006CB932100, 2009CB930400), and Chinese Academy of Sciences (KJCX2-YW-M13).

Supporting Information Available: Additional figures. This material is available free of charge *via* the Internet at http://pubs.acs.org.

REFERENCES AND NOTES

1. Zou, Y. J.; Sun, L. X.; Xu, F. Biosensor Based on Polyaniline-Prussian Blue/Multi-walled Carbon Nanotubes Hybrid Composites. *Biosens. Bioelectron.* **2007**, *22*, 2669–2674.
2. Fan, L. Z.; Hu, Y. S.; Maier, J.; Adelhelm, P.; Smarsly, B.; Antonietti, M. High Electroactivity of Polyaniline in Supercapacitors by Using a Hierarchically Porous Carbon Monolith as a Support. *Adv. Funct. Mater.* **2007**, *17*, 3083–3087.
3. Wang, Y. G.; Li, H. Q.; Xia, Y. Y. Ordered Whiskerlike Polyaniline Grown on the Surface of Mesoporous Carbon

and Its Electrochemical Capacitance Performance. *Adv. Mater.* **2006**, *18*, 2619–2623.
4. Zhang, H.; Cao, G. P.; Wang, Z. Y.; Yang, Y. S.; Shi, Z. J.; Gu, Z. N. Tube-Covering-Tube Nanostructured Polyaniline/Carbon Nanotube Array Composite Electrode with High Capacitance and Superior Rate Performance as Well as Good Cycling Stability. *Eletrochem. Commun.* **2008**, *10*, 1056–1059.
5. Zhang, H.; Cao, G. P.; Wang, W. K.; Yuan, K. G.; Xu, B.; Zhang, W. F.; Cheng, J.; Yang, Y. S. Influence of Microstructure on the Capacitive Performance of Polyaniline/Carbon Nanotube Array Composite Electrodes. *Electrochim. Acta* **2009**, *54*, 1153–1159.
6. Wang, D. W.; Li, F.; Zhao, J. P.; Ren, W. C.; Chen, Z. G.; Tan, J.; Wu, Z. S.; Gentle, I. G.; Lu, Q.; Cheng, H. M. Fabrication of Graphene/Polyaniline Composite Paper *via In Situ* Anodic Electropolymerization for High-Performance Flexible Electrode. *ACS Nano* **2009**, *3*, 1745–1752.
7. Georgakilas, V.; Gournis, D.; Tzitzios, V.; Pasquato, L.; Guldi, D. M.; Prato, M. Decorating Carbon Nanotubes with Metal or Semiconductor Nanoparticles. *J. Mater. Chem.* **2007**, *17*, 2679–2694.
8. Leschkies, K. S.; Divakar, R.; Basu, J.; Enache-Pommer, E.; Boercker, J. E.; Carter, C. B.; Kortshagen, U. R.; Norris, D. J.; Aydil, E. S. Photosensitization of ZnO Nanowires with CdSe Quantum Dots for Photovoltaic Devices. *Nano Lett.* **2007**, *7*, 1793–1798.
9. Herrikhuyzen, J. V.; George, S. J.; Vos, M. R. J.; Sommerdijk, N. A. J. M.; Ajayaghosh, A.; Meskers, S. C. J.; Schenning, A. P. H. J. Self-Assembled Hybrid Oligo(*p*-phenylenevinylene)−Gold Nanoparticle Tapes. *Angew. Chem., Int. Ed.* **2007**, *46*, 1825.
10. Wang, D. H.; Choi, D. W.; Li, J.; Yang, Z. G.; Nie, Z. M.; Kou, R.; Hu, D. H.; Wang, C. M.; Saraf, L. V.; Zhang, J. G.; Aksay, I. A.; Liu, J. Self-Assembled TiO_2-Graphene Hybrid Nanostructures for Enhanced Li-Ion Insertion. *ACS Nano* **2009**, *3*, 907–914.
11. Si, Y. C.; Samulski, E. T. Exfoliated Graphene Separated by Platinum Nanoparticles. *Chem. Mater.* **2008**, *20*, 6792–6797.
12. Wu, Z. S.; Ren, W. C.; Gao, L. B.; Zhao, J. P.; Chen, Z. P.; Liu, B. L.; Tang, D. M.; Yu, B.; Jiang, C. B.; Cheng, H. M. Synthesis of Graphene Sheets with High Electrical Conductivity and Good Thermal Stability by Hydrogen Arc Discharge Exfoliation. *ACS Nano* **2009**, *3*, 411–417.
13. Li, X. L.; Zhang, G. Y.; Bai, X. D.; Sun, X. M.; Wang, X. R.; Wang, E. G.; Dai, H. J. Highly Conducting Graphene Sheets and Langmuir−Blodgett Films. *Nat. Nanotechnol.* **2008**, *3*, 538–542.
14. Wang, H. L.; Hao, Q. L.; Yang, X. J.; Lu, L. D.; Wang, X. Graphene Oxide Doped Polyaniline for Supercapacitors. *Electrochem. Commun.* **2009**, *11*, 1158–1161.
15. Conway, B. E. *Electrochemical Supercapacitors, Scientific Fundamentals and Technological Applications*; Kluwer Academic/Plenum: New York, 1999.
16. Frackowiak, E.; Beguin, F. Carbon Materials for the Electrochemical Storage of Energy in Capacitors. *Carbon* **2001**, *39*, 937–950.
17. Wang, Y.; Shi, Z. Q.; Huang, Y.; Ma, Y. F.; Wang, C. Y.; Chen, M. M.; Chen, Y. S. Supercapacitor Devices Based on Graphene Materials. *J. Phys. Chem. C* **2009**, *113*, 13103–13107.
18. Stoller, M. D.; Park, S.; Zhu, Y. W.; An, J.; Ruoff, R. S. Graphene-Based Ultracapacitors. *Nano Lett.* **2008**, *8*, 3498–3502.
19. Rudge, A.; Davey, J.; Raistrick, I.; Gottesfeld, S. Conducting Polymers as Active Materials in Electrochemical Capacitors. *J. Power Sources* **1994**, *47*, 89–107.
20. Fusalba, F.; Gouerec, P.; Villers, D.; Belanger, D. Electrochemical Characterization of Polyaniline in Nonaqueous Electrolyte and Its Evaluation as Electrode Material for Electrochemical Supercapacitors. *J. Electrochem. Soc.* **2001**, *148*, A1–A6.
21. Zhao, G. Y.; Li, H. L. Preparation of Polyaniline Nanowire Arrayed Electrodes for Electrochemical Supercapacitors. *Microporous Mesoporous Mater.* **2008**, *110*, 590–594.
22. Gupta, V.; Miura, N. Electrochemically Deposited Polyaniline Nanowire's Network: A High-Performance Electrode Material for Redox Supercapacitor. *Electrochem. Solid-State Lett.* **2005**, *8*, A630–A632.
23. Huang, J. Y.; Wang, K.; Wei, Z. X. Conducting Polymer Nanowire Arrays with Enhanced Electrochemical Performance. *J. Mater. Chem.* **2010**, *20*, 1117–1121.
24. Wang, K.; Huang, J. Y.; Wei, Z. X. Conducting Polyaniline Nanowire Arrays for High Performance Supercapacitors. *J. Phys. Chem. C* **2010**, *114*, 8062–8067.
25. Hummers, W. S.; Offeman, R. E. Preparation of Graphitic Oxide. *J. Am. Chem. Soc.* **1958**, *80*, 1339.
26. Zu, S. Z.; Han, B. H. Aqueous Dispersion of Graphene Sheets Stabilized by Pluronic Copolymers: Formation of Supramolecular Hydrogel. *J. Phys. Chem. C* **2009**, *113*, 13651–13657.
27. Bourlinos, A. B.; Steriotis, Th. A.; Karakassides, M.; Sanakis, Y.; Tzitzios, V.; Trapalis, C.; Kouvelos, E.; Stubos, A.; Synthesis. Characterization and Gas Sorption Properties of a Molecularly-Derived Graphite Oxide-like Foam. *Carbon* **2007**, *45*, 852–857.
28. Chiou, N.-R.; Lui, C. M.; Guan, J. J.; Lee, L. J.; Epstein, A. J. Growth and Alignment of Polyaniline Nanofibres with Superhydrophobic, Superhydrophilic and Other Properties. *Nat. Nanotechnol.* **2007**, *2*, 354–357.
29. Chiou, N. R.; Epstein, A. J. Polyaniline Nanofibers Prepared by Dilute Polymerization. *Adv. Mater.* **2005**, *17*, 1679–1683.
30. Zhang, Z. M.; Wei, Z. X.; Wan., M. X. Nanostructures of Polyaniline Doped with Inorganic Acid. *Macromolecules* **2002**, *35*, 5937–5942.
31. Chen, S.; Zhu, J. W.; Wu, X. D.; Han, Q. D.; Wang, X. Graphene Oxide−MnO_2 Nanocomposites for Supercapacitors. *ACS Nano* **2010**, *4*, 2822–2830.
32. Titelman, G. I.; Gelman, V.; Bron, S.; Khalfin, R. L.; Cohen, Y.; Peled, H. B. Characteristics and Microstructure of Aqueous Colloidal Dispersions of Graphite Oxide. *Carbon* **2005**, *43*, 641–649.
33. Park, S.; Lee, K. S.; Bozoklu, G.; Cai, W. W.; Nguyen, S. T.; Ruoff, R. S. Graphene Oxide Papers Modified by Divalent Ions—Enhancing Mechanical Properties *via* Chemical Cross-Linking. *ACS Nano* **2008**, *2*, 572–578.
34. Wan, M. X.; Li, M.; Li, J. C.; Liu, Z. X. Structure and Electrical-Properties of the Oriented Polyaniline Films. *J. Appl. Polym. Sci.* **1994**, *53*, 131–139.
35. Monkman, A. P.; Adams, P. Optical and Electronic Properties of Stretch-Oriented Solution-Cast Polyaniline Films. *Synth. Met.* **1991**, *40*, 87–96.
36. Jing, X. B.; Tang, J. S.; Wang, Y.; Lei, L. C.; Wang, B. C.; Wang, F. S. Molecular Chain Structure of Doped Polyaniline. *Sci. China, Ser. B* **1990**, *33*, 787.
37. Ray, A.; Asturias, G. E.; Kersher, D. L.; Richter, A. F.; MacDiarmid, A. G.; Epstein, A. J. Polyaniline-Doping, Structure and Derivatives. *Synth. Met.* **1989**, *29*, 141–150.
38. Chiou, N. R.; Epstein, A. J. A Simple Approach To Control the Growth of Polyaniline Nanofibers. *Synth. Met.* **2005**, *153*, 69–72.
39. Kotov, N. A.; Dekany, I.; Fendler, J. H. Ultrathin Graphite Oxide−Polyelectrolyte Composites Prepared by Self-Assembly: Transition between Conductive and Non-conductive States. *Adv. Mater.* **1996**, *8*, 637–641.
40. Yang, Y. S.; Wan, M. X. Chiral Nanotubes of Polyaniline Synthesized by a Template-Free Method. *J. Mater. Chem.* **2002**, *12*, 897–901.